Passive Force-Feedback Gloves With Joint-Based Variable Impedance Using Layer Jamming

Yu Zhang, Dangxiao Wang, *Senior Member, IEEE*, Ziqi Wang, Yuru Zhang, *Senior Member, IEEE*, and Jing Xiao, *Fellow, IEEE*

***Abstract*—Force feedback gloves have a great potential in enhancing the fidelity of virtual reality and teleoperation systems. It is a challenge to develop multifinger and lightweight force feedback gloves. In this paper, we propose a solution using layer jamming sheet (LJS) on each finger joint. In simulating free space, the LJS is soft and easy to deform, which allows the finger joints to move freely with a small resistance force. In simulating constrained space, the LJS becomes stiff, which provides resistance torques to prevent the rotation of finger joints. Possible solutions for mounting the LJS on finger joints are investigated. Mechanical models of the LJS are derived by quantifying the relationship between the bending stiffness and the pressure, material, and geometry of the layer. Experiments are performed to characterize the mechanical behavior of the LJS actuator and to validate the performance of the different design solutions in simulating free space and constrained space. Experimental results indicate the potential of the proposed joint-based LJS-actuated approach in developing lightweight force feedback gloves.**

***Index Terms*—Force feedback glove, layer jamming, lightweight, soft haptics.**

I. Introduction

IMMERSIVE and light weight Head-Mounted Displays (HMD) such as Oculus Rift and HTC Vive have initiated a new era for virtual reality. Haptic feedback is becoming necessary to improve the experience of using VR systems in terms of immersion and interaction. In order to increase the immersive feeling of interaction with the virtual world, a haptic feedback device should allow users to touch and manipulate virtual objects in an intuitive and direct way by using the dexterous manipulation capabilities of our hands. Wearable force feedback gloves are a promising solution for producing immersive haptic sensation in virtual reality systems.

Another driving force of wearable force feedback gloves comes from tele-operation. For dexterous manipulation tasks using a robotic hand, it will be intuitive for a human operator to control the slave robot using a wearable force feedback glove. Compared with using a joystick or desktop haptic device such as Phantom desktop [1], using a master device such as a force feedback glove can enable more degree-of-freedom for motion control and more immersive force feedback.

In existing literature, many force feedback gloves have been developed to provide force feedback to a user's hand or fingers. According to the actuation method, they can be classified into active and passive actuation principles.

The most common active actuators are DC servo motors, such as those used in the CyberGrasp [2]. The other typical actuators are pneumatic actuators, such as those used in Rutgers Master II [3]. Other actuators include Shape Memory Alloys [4], electro-active polymers [5], [6] and artificial muscles [7]–[9] etc. The advantage of the active actuation solution is able to output active force and motion, while the disadvantage is its potential risk of injuring the fingers in the occurrence of a system failure. As actuators such as motors or pneumatic actuators are controlled to provide force feedback, the device may hurt the user's fingers if it becomes uncontrollable. To reduce the harmful effect of this failure, most of the active actuated gloves limit the maximum output force.

Different from the active actuation solution, passive gloves use a brake, controllable damper or electromagnetic clutch to provide resistance forces [10]–[14]. The user can feel the resistance force when the passive actuator is engaged. Safety is an advantage of passive actuators as passive devices would not harm the user even in the occurrence of system failures.

To get details about other force feedback gloves, refer to two recent surveys on wearable haptic devices [32], [33]. Overall, most existing force feedback gloves adopt rigid actuators and thus have limitations regarding safety and uncomfortable sensations when the rigid components directly contact users' skin. Common discomfort factors include sharp edges, rough surfaces, and the pressure exerted by the worn device [32]. Some gloves adopted rigid links and structures that are heavy and bulky, prone to causing fatigue and unsuitable to wear for a long duration [34]. Designs involving smart material and novel

Manuscript received November 16, 2018; revised March 18, 2019; accepted March 25, 2019. Date of publication April 1, 2019; date of current version September 16, 2019. This paper was recommended for publication by Associate Editor R. Raisamo upon evaluation of the reviewer's comments.This work was supported in part by the National Key Research and Development Program under Grant 2017YFB1002803 and in part by the National Natural Science Foundation of China under Grant 61631010 and Grant 61572055. *(Corresponding author: Dangxiao Wang.)*

Y. Zhang, Z. Wang, and Y. Zhang are with the State Key Laboratory of Virtual Reality Technology and Systems and Beijing Advanced Innovation Center for Biomedical Engineering, Beihang University, Beijing 100191, China. (e-mail: 13020031535@163com; wzqwzq1997@qq.com; yuru@buaa.edu.cn).

D. Wang is with the State Key Laboratory of Virtual Reality Technology and Systems and Beijing Advanced Innovation Center for Biomedical Engineering, Beihang University, Beijing 100191, China, and also with the Peng Cheng Laboratory, Shenzhen 518055, China. (e-mail: hapticwang@buaa.edu.cn).

J. Xiao is with the Robotics Engineering Program and Department of Computer Science, Worcester Polytechnic Institute, Worcester, MA 01609, USA, and also with the Beijing Advanced Innovation Center for Biomedical Engineering, Beihang University, Beijing 100191, China. (e-mail: jxiao2@wpi.edu).

Digital Object Identifier 10.1109/TOH.2019.2908636

actuation principles are needed to provide a light weighted solution for force feedback gloves.

In recent years, soft actuators such as fiber-reinforced soft bending actuators [15] and particle jamming [16] have been introduced for haptic gloves. Zhang *et al.* introduced a two-fingered force-feedback glove using pneumatic-driven soft actuators [15]. Based on the unilateral deformable features of the soft actuator using a strain-limiting layer, a dorsal-side mounting solution along with a lightweight linkage mechanism was proposed to produce fingertip force feedback. Zubrycki *et al.* and Simon *et al.* adopted particle jamming to provide resistance between fingers and palm [16], [31]. They presented two concepts using either jamming tubes or jamming pads, which could provide about 7N force feedback. They also investigated static and dynamic properties of tubes filled with different jammable materials.

Compared to partical jamming, actuators using layer jamming have the capability of simulating variable stiffness while allowing for constructing thin and lightweight form factors of a device [18]. The principle of layer jamming mechanism is to control the friction between layers of thin material, by evacuating the air pressure between the layers. Leveraging the concept of layer jamming, Choi *et al.* created a controllable, high force density, soft layer jamming brake [19]. They demonstrated that variable tensile resisting forces can be obtained through the regulation of vacuum pressure. The tensile force was measured and modeled with respect to different layer materials, vacuum pressures, and lengthening velocities. Compared to particle jamming, layer jamming has advantages in areas of thickness and responsiveness. Wall *et al.* compared the effect of granular jamming and layer jamming to achieve stiffening. The result shows that the prototype using layer jamming with two interleaved stacks of sheets achieved a stiffening factor about twice as large as the granular jamming prototypes [20].

Mitsuda introduced variable stiffness sheets using a type of layer jamming, i.e., fabric jamming [21]. The sheet could become stiff when evacuating air from the internal cavity of the sheet, and thus the sheet can simulate the sense of grasping force. However, as pointed by Mitsuda, further studies are needed on the modeling and control of layer jamming actuators to meet the contradictive requirements for simulating both free space and constrained space.

In addition to fabric jamming, other soft and rough material could also produce the layer jamming effect. It is necessary to model and measure the mechanical behavior to achieve an optimized design solution. Kim *et al.* studied both theoretically and experimentally important characteristics of layer jamming, such as stiffness and yield strength [22], [23]. An analytical model for two-layer jamming structures over major phases of deformation was derived by Narang *et al.* [24], which provided a mathematical foundation for designing layer jamming sheets.

Inspired by the potential of layer jamming actuators to formulate thin sheet structures that could be directly mounted on finger joints, in this paper, we investigate different solutions of joint-based gloves using the principle of layer jamming. The contributions of our paper include the following two aspects:

1) We quantitatively analyze the effect of the geometrical, material and mounting parameters of layer jamming actuators on the contradictive requirements for simulating both free space and constrained space. Different solutions of mounting the LJS actuator on finger joints are proposed and evaluated with considering the effect of several key variables, including the number of actuators on each finger, the mounting location, the contact mode between the LJS actuator and the hand. These results can provide quantified guidelines for designing LJS based force feedback gloves.
2) We construct analytical models on the mechanical behavior of the LJS actuator and perform experiments to measure the relationship between the evacuated air pressure, force and displacement of three LJS actuators with different material and structures. Experimental results show that the resistance torque in simulating constrained space is more than two times larger than that in simulating free space, which indicates that the thin jamming sheet with only two layers could achieve a distinct difference of resistance torques between free space and constraint space.

The remainder of this paper is organized as follows. In Section II, we introduce the principle of force feedback gloves using LJS. Design solutions of force feedback gloves using LJS are proposed in Section III. In Section IV we derive the mechanical model of the layer jamming glove. Physical prototype and experimental results are introduced in Section V and VI respectively. Conclusions and future work are provided in the Section VII.

II. Principle of Force Feedback Gloves Using LJS

A. Joint-Based Mounting Solution

According to the design choice of the fixed link, existing force feedback gloves can be classified into four types: ground-based [25], [26], dorsal-based [27], [28], palm-based [3], [29] and digit-based gloves [14], [30]. In order to provide feedback forces on the fingertip, most of these gloves normally use a transmission mechanism to transmit the actuated torque/force from actuators, like electric motors, to users' fingertip. As a result, the components of the transmission linkage introduce friction in the kinematic pairs, and increase the weight of the glove, and thus degrade the sensation of free space simulation.

To avoid the side effect of transmission mechanisms, one solution is directly mounting actuators on a user's finger joints. As illustrated in Fig. 1, LJS is mounted on each joint of the finger, like a wound plast mounted on a joint. With a thin shape and variable impedance, LJS is a promising actuating solution to construct joint-based force feedback gloves with two advantages. Firstly, without mechanical transmission mechanisms, the weight of the whole glove could be small, and the friction of the kinematic pairs could be eliminated. Secondly, as the resistance torque from each LJS can be independently controlled, it is possible to produce a resistance force with an arbitrary direction on the fingertip.

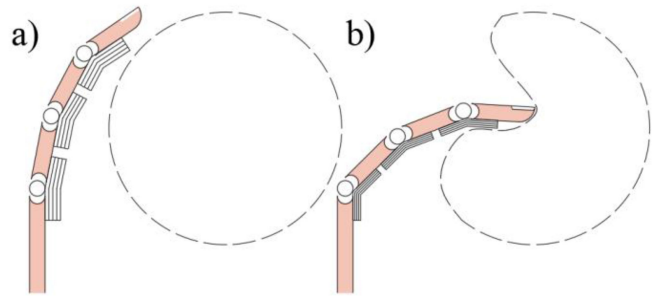

Fig. 1. Concept of the direct driven approach using joint-based layer jamming. The LJS (a) can be easily bent in free space, and (b) becomes stiff by evacuating inside air to simulate constrained space.

When the LJS is not evacuated, it can be bent freely in accordance to the finger rotation and provide a small resistance torque to the finger joints. This allows for the free space simulation.

When the LJS is evacuated, it becomes stiff and hard to be bent. When the finger joints try to rotate, it will provide a big resistance torque to the joints. This allows for the constrained space simulation.

In order to simulate diversified grasping forces and postures, it is important that the resistance torque at each finger joint could be independently controlled. Most current force feedback gloves use only one actuator on each finger to generate resistance forces [33]. For example, gloves such as Cyber Grasp typically use one wire/tendon to transmit force for each finger. When the glove generates force by using only one wire, the force applied to the fingertip is exerted in the direction that the wire pulls, which leads to a one-dimensional force exerted on fingertip. This single actuator solution cannot provide realistic feedback forces on the fingertip [35]. The reason is that, in real world grasp tasks, the contact force between each fingertip and the object is a three dimensional vector with time-varying magnitudes and directions [36]. For example, for a given grasping posture with fixed contact points, if the user intentionally changes the force magnitude, the resistance torques exerted on the three finger joints will be definitely different. Therefore, one advantage of the proposed LJS solution is able to produce a synthetic resistance force with an arbitrary direction on the fingertip.

B. Balanced Design Between Free and Constrained Space

When designing a force feedback glove, one major challenge is to meet the conflicting requirements between free space and constrained space. In free space, users' hand should feel free when a virtual hand avatar doesn't grasp any objects. Accordingly, the resistant torque of LJS needs to be as small as possible. In constrained space, we aim to simulate the sensation of grasping diverse virtual objects. The resisting torque of LJS needs to be sufficiently large to simulate touching rigid objects. Therefore, an ideal LJS should be sufficiently flexible in free space and provide a large stiffness range in constrained space.

Furthermore, the glove should provide a sufficient workspace, i.e., to allow a large rotation angle for the finger joints to simulate full closure gestures. This implies that the LJS should not interfere with the phalanges of the finger.

TABLE I
KEY PARAMETERS AND CONDITIONS OF LJS FOR DESIGNING A FORCE FEEDBACK GLOVE

Level	Category	Parameter
Parameters of a single LJS	Actuation parameters	vacuum pressure (P)
	Material parameters	Young' modulus (E)
		Friction coefficient (μ)
	Geometric Parameters	Length(L)
		Width(b)
		Thickness(h)
	Fabrication parameters	Number of layers(n)
Conditions defining the relationship between LJS and finger joints	Mounting location	Palm-side, dorsal-side, lateral-side, full-wrapped
	Contact mode	Direct contact vs. Indirect contact
	Constrained mode	Independent actuation vs. coupled actuation

As shown in previous studies [22], [24], the effect of layer jamming depends on several parameters, including friction coefficient, vacuum pressure, number of layers, and thickness of single layer etc. In order to adopt joint-based LJS for designing force feedback gloves, more parameters need to be considered for achieving a satisfied force feedback effect. In TABLE I, we summarize key parameters and conditions of LJS that need to be considered for designing a force feedback glove.

In order to increase the bending stiffness of LJS for simulating the constrained space, values of these parameters should be carefully determined. Here we analyze the effect of parameters related to a single LJS, while the effect of those parameters defining the relationship between LJS and finger joints will be elaborated in Section III.

Friction coefficient is determined by the material of the layers. In this paper, we compare two types of material (as shown in Fig. 2). One is soft fabric material (i.e., polyester fiber) obtained from a local cloth market. This type of material can easily bend to produce an excellent free space sensation. The second type of material is soft sand strip coil, which is stiffer than the fabric material and has a larger friction coefficient. The soft sand strip coil was obtained from Internet (https://m.tb.cn/h.3txy5q0). This material can produce a larger resistance torque during bending. However, its free space sensation is worse than the fabric material.

In order to produce a large resistance torque, the area of the LJS should be as large as possible. However, the area of the LJS is limited by the length and width of finger phalanges. The width of the LJS should be smaller than the width of the finger; otherwise, interference may occur between the LJSs on adjacent fingers. Furthermore, if the LJS are mounted on the

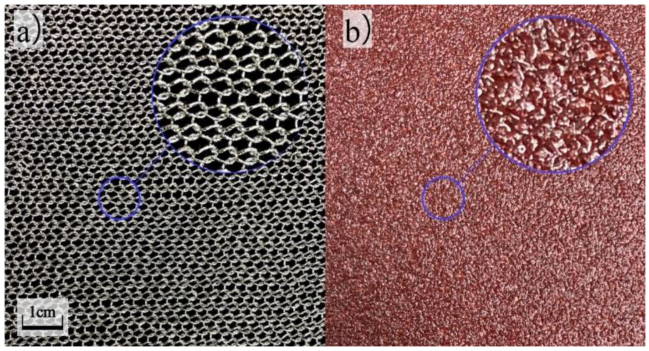

Fig. 2. Two types of layer material: fabric and soft sand strip coil.

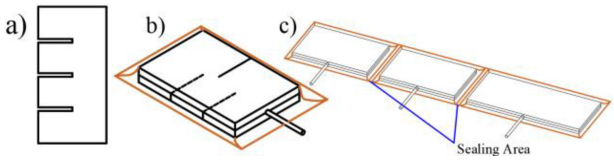

Fig. 3. Structure of LJS. (a) One layer with additional cracks to make it flexible. (b) Two layers are enclosed in an air-tight envelope. (c) Integrated structure of LJS.

palm side of finger joints, the length of the LJS should be sufficiently small to avoid potential interference between the neighboring LJSs mounted on adjacent joints. For example, when the hand is performing a grasping posture, the allowable space for the LJS actuators is becoming smaller and smaller.

In order to simulate free space sensation, the resisting torque of LJS needs to be minimized as small as possible. For the fabric material, it is sufficiently soft. However, for the soft sand strip coil, it is stiff and not easy to be bent, thus the free space sensation is poor.

To solve this problem, we introduce some cracks on the soft sand strip coil material. As shown in Fig. 3, along the length of LJS, several cracks are cut out with an equal distance. The cracks could be regarded as hinges, which could reduce the bending stiffness for simulating free space. It should be noted that the location of cracks in two adjacent layers must avoid to be collocated; otherwise, the bending stiffness of the LJS might be over-reduced, which may produce negative effects on the performance of the LJS when simulating constrained space.

Furthermore, the depth of the cracks is equal to the half width of the LJS. Through our experiments, when using a 15mm width LJS, a crack is made with 20-30mm distance. This value could keep a reasonable performance balance in both free space and constrained space.

C. Integrated Structure of LJSs on One Finger

In order to reduce the potential interference between LJS actuators for adjacent finger joints, we propose an integrated structure in which three LJSs are assembled as a whole structure. The sealing lines on the envelope are reduced from six to four, which save the space along the phalanges, as shown in Fig. 3(c). Through our experiments, keeping each LJS with

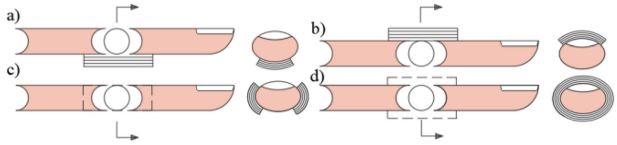

Fig. 4. The available mounting locations of LJS on a finger (Left panel: front-view. Right panel: cross-sectional view). (a) Palm-side, (b) dorsal-side, (c) lateral-side, and (d) fully-wrapped.

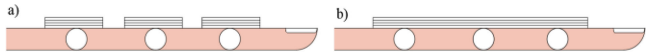

Fig. 5. The constrained modes of using LJS. (a) Single-joint dorsal-side constrained solution. (b) Multiple-joint dorsal-side constrained solution.

5mm distance is enough to ensure the sealing effect of LJSs. With the reduction of sealing areas, the length of LJS could be enlarged, which could provide a larger resisting torque. Furthermore, the air pressure within each LJS could be independently controlled, as adjacent LJSs are separated by sealing areas.

III. Mounting Solutions of LJS on Finger Joints

A. Analysis of Solution Sets of Force Feedback Gloves

There are three variables defining the possible solutions for LJS to be mounted around finger joints, including the mounting location, number of independently controlled actuators, and the contact mode between the LJS and the skin.

For the mounting location, as the LJS is used to provide resistance torques for finger joints, the possible locations of an LJS actuator with respect to its target joint include palm-side, dorsal-side, and lateral-side. Theoretically, we can combine them to obtain a fully-wrapped option. Fig. 4 summarizes all the possible locations. However, considering the interference between the fingers, only two options are preserved in our prototypes, i.e., palm-side and dorsal-side.

For the number of independently controlled actuators, there are two options. As shown in Fig. 5, for single-joint constraint, each finger joint is independently controlled by an LJS. In comparison, for multiple-joint constraint, one single LJS is used to constrain multiple joints.

There are two contact modes between the LJS and the skin, as shown in Fig. 6, direct and indirect contact. One simple way to install LJS is gluing it to a glove, like jamming tube [15]. Although this way of installation is easy for users to put on the glove, the relative movement between the hand and the glove (because of glove deformation) may degrade the force sensation. In order to allow LJS bending without perceptible clearance, the glove needs to be non-elastic and tightly contact the skin of users' hand. However, to make sure that the user can easily put a glove on and off, most gloves are elastic and thus may produce relative motion between the hand and the glove.

The other way is to install LJS directly on the fingers. One possible solution is to use Hook & Loop to make sure that LJS could be tightly clung to users' fingers.

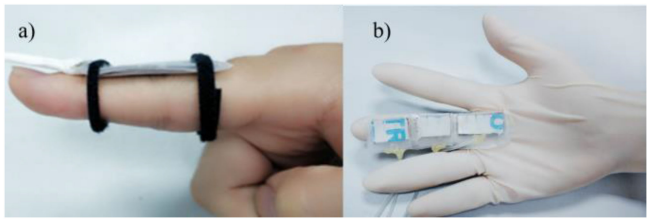

Fig. 6. Contact modes. (a) Direct contact. (b) Indirect contact.

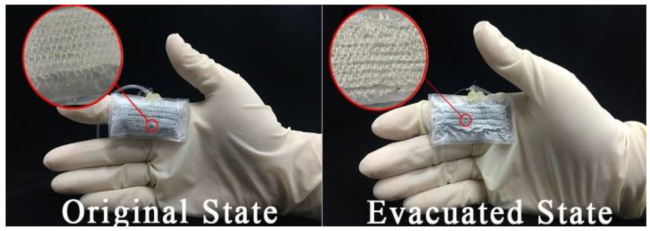

Fig. 7. The LJS in original state and evacuated state.

B. Selected Solution Sets of Force Feedback Gloves

By mounting LJS at two different locations (palm-side or dorsal-side), two different constrained modes (single-joint or multiple-joint constrained) and using two different contact modes, there would be a set of eight solutions for designing LJS-based force-feedback gloves.

For the dorsal-side plus single-joint constrained solution, as shown in Fig. 5, one advantage is that the workspace is larger compared to the palm-side mounting solution. Furthermore, another advantage is that it has a potential to install a thicker LJS than the palm-side solution. With a greater thickness, LJS would produce a larger resistance torque and thus produce a stronger grasp sensation for simulating constrained space.

However, when we install the LJSs on the dorsal-side of the finger, the force sensation for simulating grasping would be unrealistic. Because the LJS is on the dorsal side of the finger joint, the resistance torque of the sheet would be exerted on the dorsal surface of finger joint.

When the LJSs are mounted on the palm-side of the finger, the sensation for touching and grasping virtual objects is more realistic than the dorsal-side solution. However, the allowable moving angle of the finger joints is decreased, as the FJSs may interfere when the rotating angle of the finger joints is too large.

For the multiple-joint constrained solution, as shown in Fig. 5(b), one LJS is used to constrain the motion of three joints of one finger. The advantage of this solution is that only one pneumatic valve is needed to control the feedback force for each finger, and thus the cost of the control system can be reduced. However, the disadvantage is that we cannot independently control the resistance torque on each finger joint.

Another feature of this solution is that, for the palm-based mounting solution, the interference problem could be alleviated by using only one LJS on the finger compared to three LJSs.

IV. Mechanical Characteristics and Models of LJS

A. Fabrication and Mechanical Characteristics of LJS

The physical types of LJS in different states are shown in Fig. 7. When evacuating the air from LJS, the plastic envelope and the layer material will be pressed tightly. This can be used for simulating the sensation of constrained space.

As the friction between adjacent layers would hinder the movement of the layers, the bending of the sheet would be impeded. Therefore, when evacuating the air in LJS, the stiffness would increase.

When fabricating a thick and small LJS with many layers, if not using glue, the layers would be easily twisted. The bending stiffness would be decreased dramatically because of the twist. Therefore, we glued the two outermost layers of the layer material with the plastic envelope.

In the solution of [21], the fibers are covered by stretchy rubber. In our solution, we choose to cover the layer material by a nonelastic plastic envelope. The air inside the envelope is evacuated by an air tube. The edges of the envelope of LJS are sealed to make sure there is no air leakage in other areas. A capper and a glue gun are used to seal the edge of air tube and the plastic envelope.

For a vacuumed jamming structure, when vacuum is off, the structure has low bending stiffness, which is proportional to the slope of the curve between the deflection and the applied force. When vacuum is on, the structure has three deformation regimes: pre-slip, transition, and full-slip regime [24].

In pre-slip regime, the jamming structure is subjected to a small load, and the longitudinal shear stress along all regions of the interface is less than the maximum frictional stress. The jamming structure will remain entirely cohesive [24]. When the load increases, the longitudinal shear stress along some regions of the interface will equal the maximum frictional stress. Along these regions, the layers will slip, and along other regions, the layers will remain cohesive. This loading regime is called the transition regime [24]. When the load is greater than a certain threshold, the longitudinal shear stress along all regions of the interface will equal the maximum frictional stress. The jamming structure will be entirely slipped, except at regions where boundary conditions prevent slip from occurring. This loading regime is called the full-slip regime [24].

B. Mechanical Models of LJS

As the LJS is mounted on a finger joint to provide resistance torques, we need to construct mechanical models of LJS to identify the effect of design parameters on the bending torque and bending stiffness.

First, we define the bending stiffness of the LJS as the derivative of the torque versus the angle of the joint

$$k_\varphi = dM/d\varphi \tag{1}$$

where k_φ is the bending stiffness. M is the torque produced by the finger joint, and φ is the bending angle of the LJS.

The bending stiffness can be varied depending on several parameters, including the evacuated pressure, the mounting location, and the contact mode etc. In the following parts of

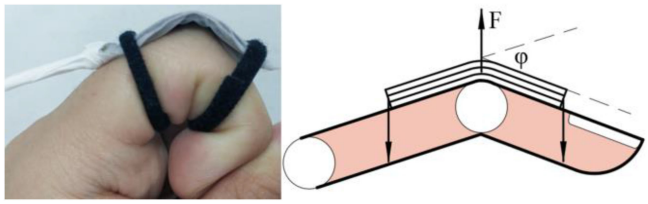

Fig. 8. Mechanical model of LJS using dorsal-side mounting direct contact mode. (a) Prototype. (b) Force analysis diagram.

this section, we will elaborate the model under the condition of *dorsal-side mounting + direct contact mode*. The mechanical models of other conditions can be derived in a similar way.

When the LJS sheet is installed on dorsal-side, as shown in Fig. 8, the force condition is similar to that in a three-point bending experiment. The torque could be computed as follows

$$\mathrm{M} = \frac{1}{4}\mathrm{FLcos}\left(\frac{\varphi}{2}\right) \tag{2}$$

where *F* refers to the force exerted on the LJS, and L is the length of LJS, as shown in Fig. 8.

It should be noted that there are two differences between our work and the model in [24]. One is the boundary condition. When the angle is small, the LJS model in our paper can be regarded as a freely supported beam under the classical three-point bending condition, instead of the cantilever beam model used in [24]. In the three-point bending condition, the longitudinal shear stress is equal in the axial direction. With increased loads, the longitudinal shear stress increases equally. When the longitudinal shear stress reaches the maximum stress, all areas start to slip, which means that there is no transition regime. The other difference is that the force is a concentrated load instead of a distributed load used in [24].

According to the mechanical models proposed in [24], as shown in Fig. 9, we derive the mechanical model for the proposed joint-based LJS actuator in the two regimes. Therefore, the force model can be derived as the follows:

$$\mathrm{F} = \begin{cases} \frac{32\mathrm{w}\left(\frac{L}{2}\right)\mathrm{Ebh}^3}{\mathrm{L}^3} & (\mathrm{Pre}-\mathrm{slip\ Regime}) \\ \frac{8\mathrm{Ebh}^3}{\mathrm{L}^3}\left(-\mathrm{w}\left(\frac{L}{2}\right)+\frac{\mu\mathrm{PL}^2}{4\mathrm{Eh}^2}\right) & (\mathrm{Full}-\mathrm{slip\ Regime}) \end{cases}. \tag{3}$$

The parameters are defined in TABLE I. Combining (2) and (3), the bending torque can be derived as

$$\mathrm{M} = \begin{cases} \frac{4Ebh^3}{3L}\varphi cos\frac{\varphi}{2} & (\mathrm{Pre}-\mathrm{slip\ Regime}) \\ \frac{Ebh^3}{3L}\left(\varphi+\frac{3\mu PL^2}{2Eh^2}\right)cos\frac{\varphi}{2} & (\mathrm{Full}-\mathrm{slip\ Regime}) \end{cases}. \tag{4}$$

Combining (1) and (4), we can derive the bending stiffness

$$\mathrm{k}_\varphi = \begin{cases} \frac{4Ebh^3}{3L}\varphi\cos\frac{\varphi}{2}-\frac{2Ebh^3}{3L}\varphi\sin\frac{\varphi}{2}\,(\mathrm{Pre}-\mathrm{slip\ Reg.}) \\ \frac{Ebh^3}{3L}\varphi\cos\frac{\varphi}{2}-\frac{Ebh^3}{6L}\varphi\sin\frac{\varphi}{2}-\frac{\mu PbhL}{4}\sin\frac{\varphi}{2}\ (\mathrm{Full}-\mathrm{slip\ Reg.}) \end{cases} \tag{5}$$

Furthermore, the transition criteria between the two regimes are as the following:

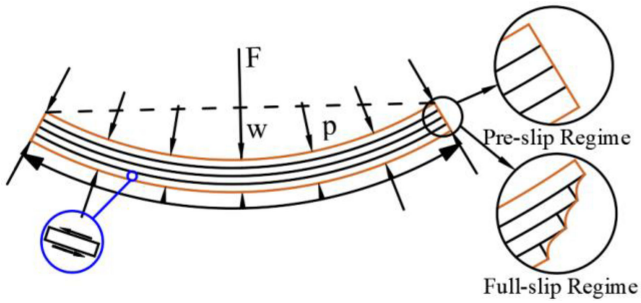

Fig. 9. Two states of LJS during a bending process.

$$\begin{cases} \mathrm{F} < \frac{8}{3}\mu\mathrm{Pbh} & (\mathrm{Pre}-\mathrm{slip\ Regime}) \\ \mathrm{F} \geq \frac{8}{3}\mu\mathrm{Pbh} & (\mathrm{Full}-\mathrm{slip\ Regime}) \end{cases}. \tag{6}$$

Furthermore, in the three-point bending condition, the deflection of the LJS sheet could be calculated as [24]:

$$\mathrm{w(x)} = \begin{cases} \frac{\mathrm{FL}^3}{8\mathrm{Ebh}^3} - \frac{3\mathrm{FL}^2\mathrm{x}}{32\mathrm{Ebh}^3} & (\mathrm{Pre}-\mathrm{slip\ Regime}) \\ \left(\frac{\mathrm{F}}{2\mathrm{Ebh}^3}-\frac{\mu\mathrm{P}}{\mathrm{Eh}^2}\right)\mathrm{x}^3+\left(\frac{3\mu\mathrm{PL}^2}{4\mathrm{Eh}^2}-\frac{3\mathrm{FL}^2}{8\mathrm{Ebh}^3}\right)\times(\mathrm{Full}-\mathrm{slip\ Regime}) \end{cases} \tag{7}$$

Combining (3) and (7), the effective stiffness (along the normal direction of the sheet) could be derived as

$$k_w = \frac{\mathrm{dF}}{\mathrm{dw}\left(\frac{\mathrm{L}}{2}\right)} = \begin{cases} \frac{32\mathrm{Ebh}^3}{\mathrm{L}^3} & (\mathrm{Pre}-\mathrm{slip\ Regime}) \\ \frac{8\mathrm{Ebh}^3}{\mathrm{L}^3} & (\mathrm{Full}-\mathrm{slip\ Regime}) \end{cases} \tag{8}$$

By changing material parameters, we can adjust Young' modulus (E) and friction coefficient (μ). As shown in the mechanical model in Eqn. (4), the bending torque of the LJS can be changed, and thus lead to different sensation in simulating free or constraint space haptic interaction. For example, the soft fabric material is easy to bend in original state and thus has an excellent free space performance but with a small bending stiffness in constraint space. In contrast, the stiffer coil material can produce a larger bending stiffness for simulating constraint space with a reduced performance in free space.

By changing geometric parameters such as length (L), width (w) and thickness (h) of each layer, as shown in the mechanical model in Eqn. (4), the bending torque of the LJS can be adjusted, which leads to the changing behavior of the glove.

By increasing the number of layers, larger bending stiffness can be obtained. However, the thickness of the actuator will increase accordingly, which may lead to potential interferences between the actuators and the palm when the fingers formulate a fully closing posture.

V. Physical Prototype of the Layer Jamming Glove

The physical prototypes of the gloves under four typical mounting conditions are shown in Fig. 10. The weights of the four solutions are 45.6g, 14.5g, 27.3g and 23.3g, respectively.

As shown in Fig. 11, the pneumatic system includes a pump with the vacuum regulator (IRV20-C8BG, SMC, Japan), electro-pneumatic regulator (ITV0090-2M*14, ITV00-03, SMC, Japan) and the filters (ZFC54*14, SMC, Japan). The vacuum

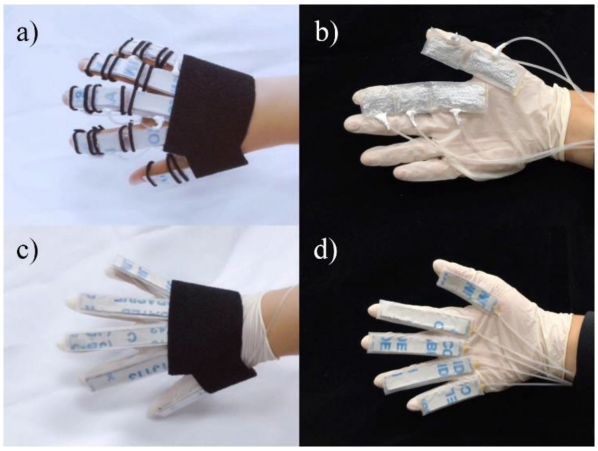

Fig. 10. The physical prototype of the force feedback gloves using LJS. (a) Dorsal-side single-joint constraint direct contact, (b) palm-side single-joint constraint indirect contact, (c) dorsal-side multiple-joint constraint indirect contact, and (d) palm-side multiple-joint constraint indirect contact.

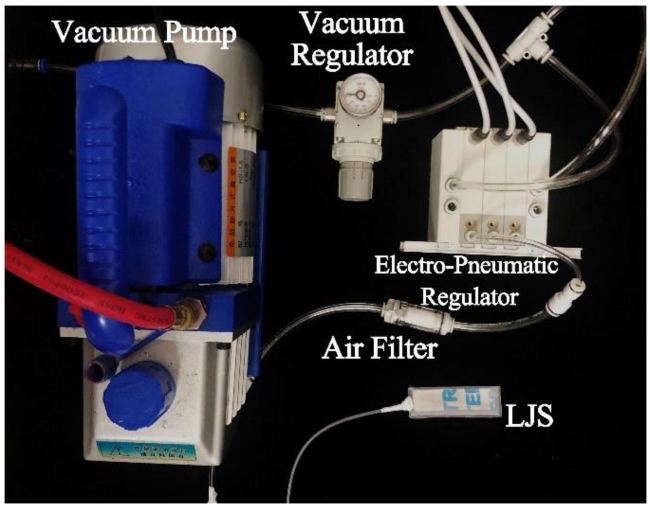

Fig. 11. The key components of the pneumatic systems.

regulator is used to statilize the pressure and the electro-pneumatic regulator is able to adjust the vacuum pressure. The filter is used to prevent the possible particles dropping into the regulator while the vacuum pressure is changing.

The low level controller is a STM32F103 microcontroller having flash memory of 512KB. The controller communicates with the PC through a serial USB port. The controller provides D/A output signals, which drive the three electro-pneumatic regulators for controlling the three LJS on each finger.

When using the proposed glove, a graphic and haptic rendering algorithm are run in PC. The virtual objects are graphically displayed through a head-mounted display. When simulating a grasping process, the finger position is recorded by motion tracking sensors, and the signals are transferred to PC. The haptic rendering algorithm computes the contact force between a hand avatar and the manipulated virtual objects, and sends the feedback force signal to drive the regulator. Then the LJS would be evacuated and become rigid, so that a user could feel force feedback.

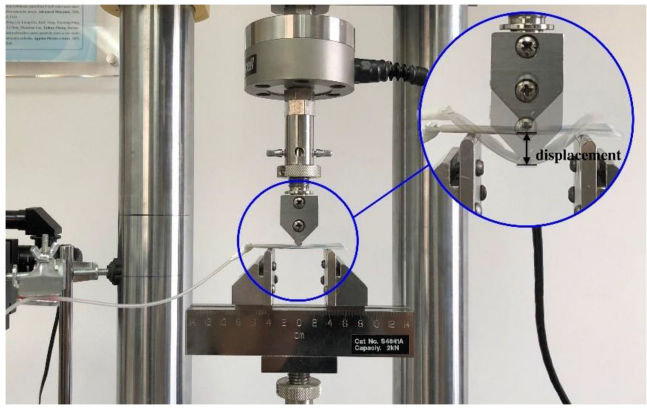

Fig. 12. The experimental scenario of exerting load on a LJS sheet.

Furthermore, we need to construct the model between the target joint torque and the evacuated air pressure, which is necessary for real time control. When finger joints rotate, the LJS provides the resistance torque. For a designated LJS, the number of layers, length, width, and thickness is constant. The only controllable parameter is vacuum pressure. Based on (4), the pressure could be computed as follows:

$$\mathrm{p} = \left(2\mathrm{M} - \frac{\mathrm{Ebh}^3}{\mathrm{L}}\sin\varphi\right) / \left(\mu bhcos\frac{\varphi}{2}\right). \tag{9}$$

VI. Performance Analysis

A. Experiments on Characterizing the LJS

Three types of LJS were tested to obtain the relationship between bending stiffness and vacuum pressure. One is made by soft sand strip coil without cracks, so we named it as *standard LJS*. Another LJS is made by soft sand strip coil with cracks, which is called as *crack LJS*. The third one is made by fabric that is called as *fabric LJS*. All LJSs' length is 60mm. This value is equal to the length of LJS installed on dorsal-side of metacarpal joint of middle finger. The first two LJSs have the same thickness of 1.78mm with a 15mm width. The third LJS has a thickness of 4.66mm and a 30mm width.

As shown in Fig. 12, a universal tensile testing machine (Instron 5848 Micro Tester, $\pm$250N, Instron Inc., US) is used to exert a load in the middle of LJS at a uniform speed of 0.5mm/s. The span between the two supported points is set as 40mm. The machine is able to ensure the expected relationship between force and displacement. The sample frequency is 100Hz, and the travel distance of loading is 15mm. The displacement in Fig. 13 refers to the vertical displacement of the center of the LJS, i.e., the displacement of the contact point between the LJS and the indenter of the testing machine.

The relationship between the exerted force and the displacement of the three LJSs are shown as Fig. 13 a), b) and c), respectively. Several important characteristics can be observed from these curves.

First, for a given displacement, the resistance force is increasing with the increase of the vacuum pressure. The results

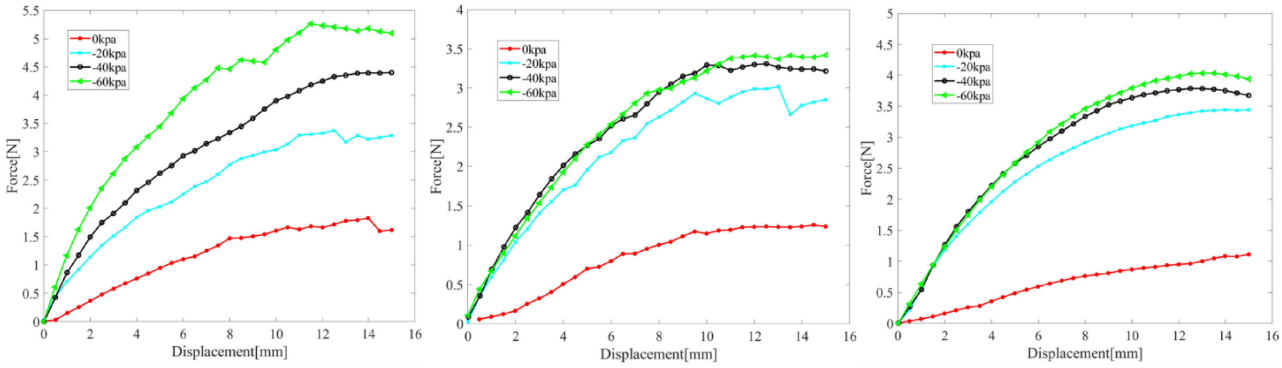

Fig. 13. The results of experiment. Mechanical behavior of (a) standard LJS, (b) crack LJS, and (c) fabric LJS.

show that the manufactured LJS sheet can change its resistance force with respect to the increase of the vacuum pressure.

Second, for a given vacuum pressure, the results show a nonlinear relationship between the exerted force and the displacement. The slope of the curve is big when the displacement is small, and then suddenly decreases along with the increase of the displacement. The slope repre-sents the stiffness of the LJS sheet as defined in (8). The transition point separating the pre-slip and full-slip regimes can be found on each curve based on the slope of the curve.

For example, in Fig. 13, in the pre-slip regime, the stiffness is almost constant. When the displacement is large enough, the LJS is working in the full-slip regime. At this time, the stiffness becomes much smaller than that of the pre-slip regime.

In addition, in the pre-slip regime, the curves of vacuumed states become overlapped, which means that the vacuum pressure does not influence the curve. This result validates the model in (3), which states that the resistance force in the pre-slip regime is independent of the vacuum pressure. In contrary, in the full-slip regime, the forces increase with the increase of vacuum pressure.

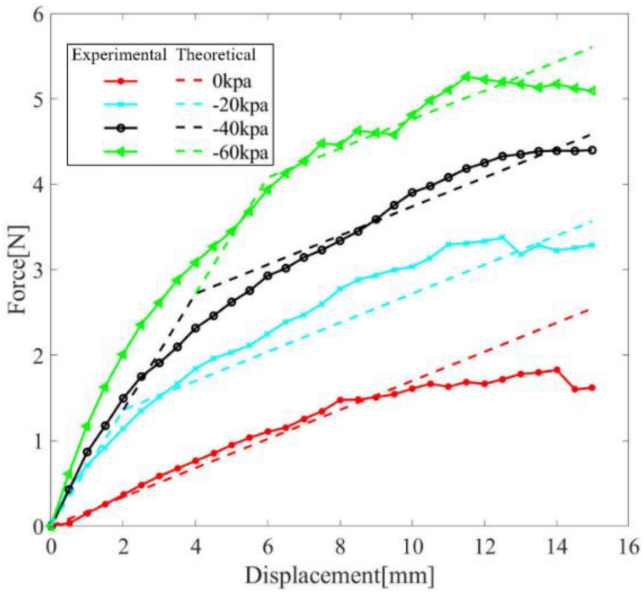

Fig. 14. Comparison of the force-displacement profiles between theoretical and experimental results.

The effect of the layer material can be observed from the comparison of the three LJSs. As for the standard LJS, because the elasticity modulus and friction coefficient of soft sand strip coil are much larger than the fabric LJS, when providing the same force feedback, a smaller geometric size is needed.

The crack LJS's layers used the same material with standard LJS, but it was cut off with cracks. With these cracks, its stiffness and elasticity modulus in both states were reduced. Based on (3) and (4), for a given vacuum pressure, the force feedback it could provide is much smaller than the standard LJS, as shown in comparison between the force values in Fig. 13.

Among the three type of actuators used in the experiments, we chose *standard LJS* to analyze the error between the theoretical model and experimental results. The main reason is that our theoretical model is targeting the modeling the mechanical behavior of two layered material, which is consistent with the number of layers in the *standard LJS*. By fitting the curves in Fig. 13(a) using regression analysis, the Young's modulus (E) and the friction coefficient (μ) are estimated as 419.8 Mpa and 1.9 respectively. Then, based on the models in Section IV.B, we obtain the theoretical results (shown in dashed lines) in Fig. 14. The shape of the slope of these results are consistent with those experimentally obtained slopes.

Taking the fabric LJS as an example, based on the curves in Fig. 13(c), we compute the values of the slope (i.e., the stiffness of the two regimes) and the value of the transition displacement (w_t) between the two regimes. We distinguish and define the pre-slip and full-slip regime by computing the slope of the force-displacement curve. The location of the transition displacement is where the slopes change dramatically. When the fluctuation error between the adjacent sampling points is smaller than 10%, we classify this region as belonging to the constant slope region. In the meantime, we calculated R2 (regression coefficient) in different position to make sure each R2 is as large as possible. The results for each vacuum pressure are summarized in TABLE II. For a given vacuum pressure, all stiffness values of the pre-slip regime are about four times than that of the full-slip regime. The regression coefficient (R2) shows that these data are reliable. The value of transition displacement is quite linear with respect to the vacuum pressure

TABLE II
STIFFNESS AND TRANSITION POINTS OF FABRIC LJS IN EACH VACUUM PRESSURE

Vacuum pressure [-kpa]	Stiffness of the pre-slip regime		Stiffness of the full-slip regime		Transition displacement
	k_1 [N/mm]	R^2	k_2 [N/mm]	R^2	w_t [mm]
0	-	-	0.08	0.97	0
20	0.47	0.98	0.12	0.92	5
40	0.39	0.97	0.12	0.84	6
60	0.40	0.97	0.09	0.97	9

and its regression coefficient is 0.92. Even in much more layers' structure of jamming, the stiffness is still constant in pre-slip regime and full-slip regime, respectively. And the relationship of the regimes may still be four times.

As shown in [24], the governing equations of the jamming structure are derived by using Euler-Bernoulli beam theory, with the assumption of the layers are elastic and isotropic. In Fig. 12(a) and (b), there is no overlap for the force-displacement curves under different air pressure, which might be caused by the physical characteristics of the material used. In these two figures, the LJS actuators are made of soft sand strip coil, which is not strictly elastic and isotropic. This might be the reason that caused the difference between the experimental results and the theoretic model. Nevertheless, the slope of all the curves in Fig. 12a) and b) manifests a nearly constant value either in the pre-slip regime or in the full-slip regime, which validates the constant stiffness model in Eqn. (8).

B. Performance in Free Space and Constrained Space

In this section, we aim to measure the force feedback performance of the LJS when it is integrated with a rotating finger joint. Because it is hard to directly measure the resistance torque of the LJS, we propose a solution to measure the fingertip force and then compute the resistance torque.

As shown in Fig. 15, we fix one end of a two-phalange low-friction wooden hand with a fixture. Next, a force sensor (FSG15N1A, Honeywell Inc., US) is mounted on the dorsal side of the fingertip. A user moves the force sensor to push the finger nail. The force sensor is slowly moved at a constant rotating speed and is always perpendicular to the distal phalange. The force signal under different vacuum degrees and different joint angles are measured. In order to make sure the force sensor is always kept perpendicular to the distal phalange, a coordinate paper and a protractor are utilized to measure the angle before each measurement. Then the joint torque is calculated by multiplying the force signal with the length of the distal phalange. For each air pressure, the measurement process is repeated for three times and an average torque is calculated. The measured LJS has two layers with 1.78mm thickness, 30mm length and 15mm width.

Fig. 16(a) illustrates the relationship between joint torque and angle in the dorsal-side plus single joint constraint solution. With the increase of vacuum pressure and joint angle, the joint torque increases. The maximum feedback torque is 74.5N·mm

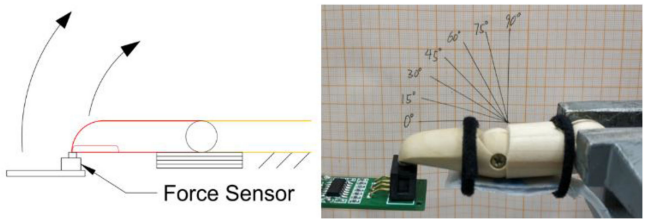

Fig. 15. Experiment for measuring the output force of LJS.

(when vacuum pressure is 80kpa). In free space (when vacuum pressure is 0kpa), the maximum resistant torque is 29N·mm. The results indicate that this solution could achieve a distinct difference of resistance torques between free space and constrained space. An accompanied video provides the real time interaction process of our developed LJS-based gloves using the four different solutions shown in Fig. 10.

Fig. 16(b) illustrates the relationship between joint torque and angle in the palm-side single joint constraint solution. For each vacuum pressure, the joint torque is proportional to the joint angle. In free space, the maximum of the joint torque is 29.1N·mm, and in constrained space the maximum of the joint torque is 77.0N·mm. Fig. 16(c) shows the relationship between fingertip force and vacuum degree of the multiple-joint constrained solution. When we use one LJS to constrain the movement of all three joints, we could use fewer regulators. For a given pressure, the palm-side solution could provide a larger feedback force than the dorsal-side solution in both free space and constrained space.

The pros and cons of the proposed mounting solutions could be compared based on experimental results. For the dorsal-side mounting and direct contact mode, reliable torque feedback can be provided. However, one disadvantage is the unnatural sensation of the force exerted on the dorsal surface of the knuckle. In contrary, if the LJS is installed directly on the palm side, the LJSs could interfere with each other when the hand is closing. In the indirect contact mode, LJS actuators are glued on a latex glove. Compared to the direct contact mode, this mode is easy for user to put on and put off the glove. However, the disadvantage is that the deformation of the glove could reduce the torque feedback sensation of LJS. When the user's finger bends in the simulated constrained space, LJS would not be bent easily. Because the latex glove is elastic, the angle of the LJS is much smaller than the angle of the finger joint. This problem is more severe for the soft sand strip coil layer material with a large stiffness, even using the LJS with cracks. When LJS is in the palm-side with the glove, then in the constrained space, there are gaps/clearances between fingers and LJS.

C. Discussions

Our experimental results show that the resistance torque of the constraint space is more than two times greater than the resistance torque in simulating free space, which indicate that the thin jamming sheet with only two layers could achieve a distinct difference of resistance torques between free space and constrained space. Compared to classic solutions using active

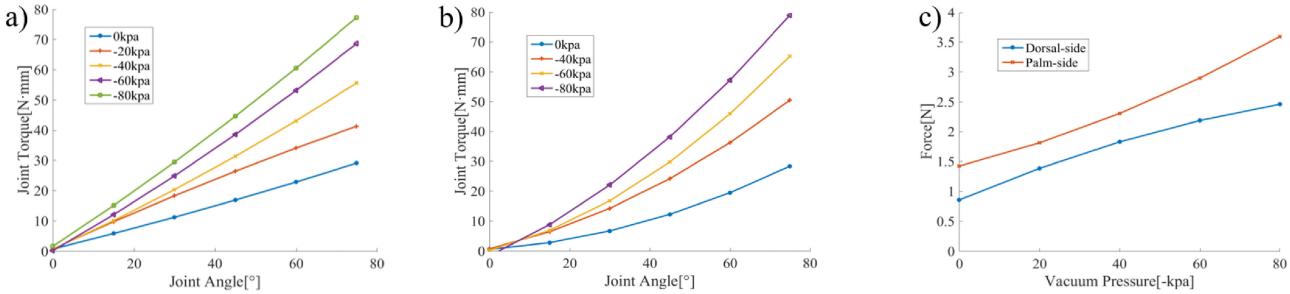

Fig. 16. The experiments of gloves. Relationship between joint angle and joint torque in (a) dorsal-side and (b) palm-side single-joint constrained solution. (c) Relationship between maximal force and vacuum pressure in multiple-joint constrained solution.

actuators and transmission mechanisms, the proposed solution is lightweight and can ensure inherent safety because of the passive actuation principle. Furthermore, by independently controlling the resistance torque from each LJS, the proposed solution is able to produce a synthetic resistance force with an arbitrary direction on the fingertip.

While our work is inspired by previous studies on jamming-based gloves [21], [31], we systematically investigated how the contradictive requirements from free space and constrained space can be compromised by selecting different geometrical, material and mounting parameters. For example, in previous jamming tube solution, 100 layers of materials was enclosed in the jamming structure. In our design, only two layers of materials are enclosed in the jamming structure. Our results show that the selection of material can significantly change the jamming effect.

Using fewer layers, the thickness of the LJS actuator can be reduced and thus to maintain a compact structure to avoid interference between the actuator and the finger during grasping process.

In the paper of Mitsuda [21], only a preliminary concept of using layer jamming for force feedback gloves is discussed. There was no quantified modeling and experimental validation on the mechanical behavior of the LJS actuators. In our study, we constructed analytical models on the mechanical behavior of the LJS and performed experimental measurements to observe the relationship between the evacuated air pressure, force and displacement of three LJS actuators with different material and structures.

Furthermore, different solutions of mounting the LJS actuator on users' fingers are proposed and evaluated in our paper. In [31], for each finger, one jamming tube is used to constrain the motion of all finger joints. This solution is the same as the palm-side multiple-joints constraint solution in our work. In addition to this solution, we compared the advantages and disadvantages of other three different mounting solutions for mounting layer jamming actuators on finger joints. The comparisons of the four mounting solutions indicate that each solution has its pros and cons, while users should select appropriate solutions for different application scenarios. These results can provide quantified guidelines for designing LJS based force feedback gloves.

In addition to the advantage of the proposed LJS solution, several limitations were found based on our study. One limitation is the limited life cycle. We performed pilot experiments to test the number of cycles for the layer jamming sheet. For the fabric material, it is about 100 cycles before the material get fatigued. For the sand paper material, it is about 40-60 cycles before the material get fatigued. In the future, we need to find new materials to enlarge the lifespan of the jamming actuators.

The other limitation is the inability to simulate releasing process. When the layer jamming sheet is evacuated, it behaves plastically under external torque. In other words, the deformation increases during the loading process, and the deformation does not decrease during unloading process, unless there is an external torque to make it return to the original shape. Actually, the layer jamming sheet belongs to passive actuators. Like other passive actuators such as brakes, the LJS can only simulate force feedback when the user tries to increase grasping force on a virtual object, and it cannot simulate the decreasing force during object releasing.

Another limitation of the proposed glove is that the latency of the whole system is about 200ms-300ms, which is mainly caused by the delay of regulators and the time cost of air flow from the pump to the LJS. The error of LJS in three-point bending experiment is about 5%, which implies a fairly good reproducibility of force output.

The output force when attaching on human's finger might be different depending on wearer's finger size. With different length of each finger segment, the equivalent force on users' fingertip will be varied.

Furthermore, the position where the LJS is attached may affect the resistance torque as well. Our mechanical model is defined with respect to the center of the LJS. However, if the center of the LJS is not coincident with the center of the target joint (this situation might occur because of mounting error), the actual output torque is different from the theoretical one. In the future, personalized calibration methods need to be explored to reduce the error.

VII. Conclusions and Future Work

In this paper, we investigate different solutions of using layer jamming sheet (LJS) on each finger joint for designing force feedback gloves. Key parameters of LJS are summarized and their effect on free space and constrained space are analyzed. Novel fabrication approaches are proposed, including improving the free space performance by introducing cracks

and enlarging the stiffness of LJS by gluing the outermost layers with the envelope.

To fulfill the proposed joint-based actuating concept, we introduce several solutions of mounting LJS on finger joints with consideration of several design factors, including number of actuators on each finger, mounting location, contact mode between the LJS and the hand. Mechanical models of the LJS actuator are derived to quantify the effect of design variables on bending torque and bending stiffness, including the evacuated air pressure, the bending angle of the actuator, the frictional coefficient of the layer material, the number of layers, and the geometrical parameters of the layers etc.

Experimental results show that the proposed solutions could ensure backdrivability in free space and produce a large range of resistance torque in simulating constrained space. For all proposed solutions, the frictional torque in simulating the free space is much smaller than the maximum torque in simulating the constrained space. The weight of the four prototypes in Fig. 10 is less than 50g. These results indicate that the proposed joint-based LJS actuating concept has the potential in developing light weighted force feedback gloves for future virtual reality or teleoperation applications.

Future work includes improving LJS by using novel materials to produce a larger range of variable impedance and to make the LJS thinner. Motion tracking sensors will be integrated with the LJS-based glove to enable full haptic interaction capabilities. In addition, the LJS-based glove only provides passive forces; it is an interesting topic to combine this actuator with active force feedback solutions to develop more powerful force feedback gloves.

REFERENCES

[1] K. Salisbury, D. Brock, T. Massie, N. Swarup, and C. Zilles, "Haptic rendering: Programming touch interaction with virtual objects," in *Proc. Symp. Interactive 3D Graph.*, Apr. 1995, pp. 123–130.

[2] CyberGlove Systems. (2013) Cybergrasp. [Online]. Available: http://www.cyberglovesystems.com/

[3] M. Bouzit, G. Burdea, G. Popescu, and R. Boian, "The rutgers master II-new design force-feedback glove," *IEEE/ASME Trans. Mechatronics*, vol. 7, no. 2, pp. 256–263, Jun. 2002.

[4] Y. Kuroda, S. Yu, M. Imura, Y. Uranishi, and O. Oshiro, "Haptic glove using compression-induced friction torque," in *Proc. ASME Dyn. Syst. Control Conf.*, Oct. 2013, pp. 455–478.

[5] I. M. Koo, K. Jung, J. C. Koo, J. D. Nam, Y. K. Lee, and H. R. Choi, "Development of soft-actuator-based wearable tactile display," *IEEE Trans. Robot.*, vol. 24, no. 3, pp. 549–558, Jun. 2008.

[6] H. S. Lee et al., "Design analysis and fabrication of arrayed tactile display based on dielectric elastomer actuator," *Sensors Actuators A Physical*, vol. 205, pp. 191–198, Jan. 2014.

[7] K. Tadano, M. Akai, K. Kadota, and K. Kawashima, "Development of grip amplified glove using bi-articular mechanism with pneumatic artificial rubber muscle," in *Proc. IEEE Int. Conf. Robot. Autom.*, May 2010, pp. 2363–2368.

[8] D. Ryu, K. W. Moon, H. Nam, and Y. Lee, "Micro hydraulic system using slim artificial muscles for a wearable haptic glove," in *Proc. IEEE/RSJ Int. Conf. Intell. Robots Syst.*, Sep. 2008, pp. 3028–3033.

[9] Z. Sun, X. Miao, and X. Li, "Design of a bidirectional force feedback dataglove based on pneumatic artificial muscles," in *Proc. Int. Conf. Mechatronics Autom.*, Aug. 2009, pp. 1767–1771.

[10] T. Koyama, I. Yamano, K. Takemura, and T. Maeno, "Multi-fingered exoskeleton haptic device using passive force feedback for dexterous teleoperation," in *Proc. IEEE/RSJ Int. Conf. Intell. Robots Syst.*, 2002, pp. 2905–2910, vol. 3.

[11] S. H. Winter and M. Bouzit, "Use of magnetorheological fluid in a force feedback glove," *IEEE Trans. Neural Syst. Rehabil. Eng.*, vol. 15, no. 1, pp. 2–8, Mar. 2007.

[12] J. Blake and H. B. Gurocak, "Haptic glove with MR brakes for virtual reality," *IEEE/ASME Trans. Mechatronics*, vol. 14, no. 5, pp. 606–615, Oct. 2009.

[13] K. I. Koyanagi, Y. Fujii, and J. Furusho, "Development of VR-STEF system with force display glove system," in *Proc. Int. Conf. Augmented Tele-Existence*, Dec. 2005, pp. 91–97.

[14] I. Choi, E. W. Hawkes, D. L. Christensen, C. J. Ploch, and S. Follmer, "Wolverine: A wearable haptic interface for grasping in virtual reality," in *Proc. IEEE/RSJ Int. Conf. Intell. Robots Syst.*, Dec. 2016, pp. 986–993.

[15] Y. Zhang, D. Wang, Z. Wang, Y. Wang, L. Wen, and Y. Zhang, "A two-fingered force feedback glove using soft actuators," in *Proc. IEEE Haptics Symp.*, Mar. 2018, pp. 186–191.

[16] I. Zubrycki and G. Granosik, "Novel haptic glove-based interface using jamming principle," in *Proc. 10th Int. Workshop Robot. Motion Control*, pp. 46–51, Jul. 2015.

[17] T. M. Simon, R. T. Smith, and B. H. Thomas, "Wearable jamming mitten for virtual environment haptics," in *Proc. ACM Int. Symp. Wearable Comput.*, Sep. 2014, pp. 67–70.

[18] J. Ou, L. Yao, D. Tauber, J. Steimle, R. Niiyama, and H. Ishii, "jamSheets: Thin interfaces with tunable stiffness enabled by layer jamming," in *Proc. 8th Int. Conf. Tangible, Embedded Embodied Interact.*, Feb. 2014, pp. 65–72.

[19] I. Choi, N. Corson, L. Peiros, E. W. Hawkes, S. Keller, and S. Follmer, "A soft, controllable, high force density linear brake utilizing layer jamming," *IEEE Robot. Autom. Lett.*, vol. 3, no. 1, pp. 450–457, Jan. 2018.

[20] V. Wall, R. Deimel, and O. Brock, "Selective stiffening of soft actuators based on jamming," in *Proc. IEEE Int. Conf. Robot. Autom.*, May 2015, pp. 252–257.

[21] T. Mitsuda, "Variable-stiffness sheets obtained using fabric jamming and their applications in force displays," in *Proc. IEEE World Haptics Conf.*, Jun. 2017, pp. 364–369.

[22] Y.-J. Kim, S. Cheng, S. Kim, and K. Iagnemma, "A novel layer jamming mechanism with tunable stiffness capability for minimally invasive surgery," *IEEE Trans. Robot.*, vol. 29, no. 4, pp. 1031–1042, Aug. 2013.

[23] Y.-J. Kim, S. Cheng, S. Kim, and K. Iagnemma, "Design of a tubular snake-like manipulator with stiffening capability by layer jamming," in *Proc. IEEE/RSJ Int. Conf. Intell. Robots Syst.*, Oct. 2012, pp. 4251–4256.

[24] Y. S. Narang, J. J. Vlassak, and R. D. Howe, "Mechanically versatile soft machines through laminar jamming," *Adv. Functional Mater.*, vol. 28, 2018, Art. no. 1707136.

[25] T. Endo et al., "Five-fingered haptic interface robot: HIRO III," *IEEE Trans. Haptics*, vol. 4, no. 1, pp. 14–27, Jan.-Mar. 2011.

[26] L. Liu, S. Miyake, K. Akahane, and M. Sato, "Development of string-based multi-finger haptic interface SPIDAR-MF," in *Proc. 23rd Int. Conf. Artif. Reality Telexistence*, pp. 67–71, Dec. 2013.

[27] S. H. Winter and M. Bouzit, "Use of magnetorheological fluid in a force feedback glove," *IEEE Trans. Neural Syst. Rehabil. Eng.*, vol. 15, no. 1, pp. 2–8, Mar. 2007.

[28] J. Blake and H. B. Gurocak, "Haptic glove with MR brakes for virtual reality," *IEEE/ASME Trans. Mechatronics*, vol. 14, no. 5, pp. 606–615, Oct. 2009.

[29] I. Sarakoglou, A. Brygo, D. Mazzanti, N. G. Hernandez, D. G. Caldwell, and N. G. Tsagarakis, "HEXOTRAC: A highly under-actuated hand exoskeleton for finger tracking and force feedback," in *Proc. IEEE/RSJ Int. Conf. Intell. Robots Syst.*, Oct. 2016, pp. 1033–1040.

[30] R. Zhang, A. Kunz, P. Lochmatter, and G. Kovacs, "Dielectric elastomer spring roll actuators for a portable force feedback device," in *Proc. 14th Symp. Haptic Interfaces Virtual Environ. Teleoperator Syst.*, Mar. 2016, pp. 347–353.

[31] I. Zubrycki and G. Granosik, "Novel haptic device using jamming principle for providing kinaesthetic feedback in glove-based control interface," *J. Intell. Robot. Syst.*, vol. 85, no. 3/4, pp. 1–17, 2017.

[32] C. Pacchierotti, S. Sinclair, M. Solazzi, A. Frisoli, V. Hayward, and D. Prattichizzo, "Wearable haptic systems for the fingertip and the hand: Taxonomy, review, and perspectives," *IEEE Trans. Haptics*, vol. 10, no. 4, pp. 580–600, Oct.–Dec. 2017.

[33] D. Wang, M. Song, A. Naqash, Y. Zheng, W. Xu, and Y. Zhang, "Toward whole-hand kinesthetic feedback: A survey of force feedback gloves," *IEEE Trans. Haptics*, to be published., doi: 10.1109/TOH.2018.2879812.

[34] S. H. Winter and M. Bouzit, "Testing and usability evaluation of the MRAGES force feedback glove," in *Proc. Int. Workshop Virtual Rehabil.*, 2006, pp. 82–87.

[35] A. Frisoli, F. Simoncini, M. Bergamasco, and F. Salsedo, "Kinematic design of a two contact points haptic interface for the thumb and index fingers of the hand," *J. Mech. Des.*, vol. 129, pp. 520–529, 2007.
[36] T. Feix, I. M. Bullock, and A. M. Dollar, "Analysis of human grasping behavior: Object characteristics and grasp type," *IEEE Trans. Haptics*, vol. 7, no. 3, pp. 311–323, Jul.–Sep. 2014.

Yu Zhang was born in Hunchun, China. He received the B.S. degree from the School of Energy and Power Engineering, Beihang University, Beijing, China, in 2018. His research interests include robotics, human machine interaction, and haptic device.

Dangxiao Wang (M'05–SM'13) received the Ph.D. degree from Beihang University, Beijing, China, in 2004. He is currently a Professor at the State Key Laboratory of Virtual Reality Technology and Systems, Beihang University. From 2006 to 2016, he was an Assistant and Associate Professor in the School of Mechanical Engineering and Automation, Beihang University. His research interests include haptic rendering, NeuroHaptics, and medical robotic systems. He has been an Associate Editor of the IEEE TRANSACTIONS ON HAPTICS since 2015. He was the Chair of the Executive Committee of the IEEE Technical Committee on Haptics from 2014 to 2017.

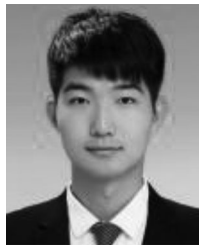

Ziqi Wang was born in Xinzhou, China. He received the B.S. degree from the School of Mechanical Engineering and Automation, Beihang University, Beijing, China, in 2018. He is currently working toward the M.E. degree at the School of Mechanical Engineering and Automation, Beihang University, China. His research interests include virtual reality, human–machine interaction, and haptic device.

Yuru Zhang (M'95–SM'08) received the Ph.D. degree in mechanical engineering from Beihang University, Beijing, China, in 1987. She is currently a Professor at the State Key Laboratory of Virtual Reality Technology and Systems, Beihang University. Her technical interests include haptic human-machine interface, medical robotic systems, robotic dexterous manipulation, and virtual prototyping. She is a member of ASME.

Jing Xiao received the Ph.D. degree in computer, information, and control engineering from the University of Michigan, Ann Arbor, MI, USA. She is the Deans' Excellence Professor, William B. Smith Distinguished Fellow in Robotics Engineering, a Professor of computer science, and the Director of the Robotics Engineering Program, Worcester Polytechnic Institute (WPI). She joined WPI from the University of North Carolina at Charlotte. Her research spans robotics, haptics, and intelligent systems. She has coauthored a monograph, holds one patent, and published extensively in major robotics journals, conferences, and books. She is the recipient of the 2015 Faculty Outstanding Research Award of the College of Computing and Informatics, University of North Carolina at Charlotte.